Stanford Exploration Project, Report 112, November 11, 2002, pages 123–131

Short Note

Multicomponent Stolt residual migration: a real data example

Daniel Rosales [1]

INTRODUCTION

Residual migration is the process of updating an image without re-running the entire migration process. Its main application is in refining of velocity models. Rosales et al. (2001) first introduced Stolt residual migration for converted waves (*PS*).

Stolt migration is a constant velocity process. Although Stolt residual migration is also based on the assumption of constant velocity, Sava (2000) shows that Stolt residual migration is valid in variant velocity media, since the residual migration operator depends only on the ratio between the migration velocity and the real velocity.

For converted waves, Stolt residual migration basically depends on the combination of three out of four parameters: 1) The ratio between the migration and the real *P*-velocity (ρ_p), 2) the ratio between the migration and the real *S*-velocity (ρ_s), 3) the ratio between the *P* and *S* migration velocities (γ_0) and 4) the ratio between the real *P* and *S* velocities (γ).

Understanding how these parameters interact and affect *PS* residual migration in a non-constant velocity medium is of crucial importance for future velocity analysis studies. I present residual migration results on a 2D line extracted from the 3D OBC data set of the Alba field after geometry regularization (Rosales and Biondi, 2002).

THEORY REVIEW

Rosales et al. (2001) describe three possible ways to perform residual migration. The most precise method is an exact derivation which involves the combination of the ρ_p, ρ_s and γ_0 parameters. This method attempts to simultaneously correct the effect of two inaccurate velocity fields.

Assuming that the initial migration was done with the velocities v_{0p} and v_{0s}, and that the

[1] **email:** daniel@sep.stanford.edu

correct velocities are v_{mp} and v_{ms}, we can then write

$$\left\{ \begin{array}{l} k_{z_0} = \frac{1}{2}\left(\sqrt{\frac{\omega^2}{v_{0p}^2} - k_s^2} + \sqrt{\frac{\omega^2}{v_{0s}^2} - k_g^2}\right) \\ k_{z_m} = \frac{1}{2}\left(\sqrt{\frac{\omega^2}{v_{mp}^2} - k_s^2} + \sqrt{\frac{\omega^2}{v_{ms}^2} - k_g^2}\right). \end{array} \right. \tag{1}$$

Solving for ω^2 in the first equation of (1) and substituting it in the second equation of (1), we obtain the expression for prestack Stolt depth residual migration for converted waves:

$$k_{z_m} = \frac{1}{2}\sqrt{\rho_p^2 {\kappa_0}^2 - k_s^2} + \frac{1}{2}\sqrt{\rho_s^2 {\gamma_0}^2 {\kappa_0}^2 - k_g^2}, \tag{2}$$

where ${\kappa_0}^2$ is the transformation kernel defined as:

$${\kappa_0}^2 = \frac{4({\gamma_0}^2+1){k_{z_0}}^2 + ({\gamma_0}^2-1)({k_g}^2 - {k_s}^2) - 4k_{z_0}\sqrt{(1-{\gamma_0}^2)({\gamma_0}^2{k_s}^2 - {k_g}^2) + 4{\gamma_0}^2{k_{z_0}}^2}}{({\gamma_0}^2-1)^2},$$

and $\rho_p = \frac{v_{0p}}{v_{mp}}$, $\rho_s = \frac{v_{0s}}{v_{ms}}$, and $\gamma_0 = \frac{v_0 p}{v_0 s}$.

This formulation depends only on velocity ratios. This fact implies that it is a valid formulation for non-constant velocity media, as suggested by Sava (2000).

Methodology

Residual migration is a very useful tool for velocity analysis. Even though it is based on a constant velocity media, the residual migration depends only on velocity ratios. Therefore, it is approximately correct and applicable for variable velocity models, at least with depth migration.

Since I handle Stolt residual migration for converted waves using three parameters, it is important to simplify the problem. The more parameters we have to search for, the more complicated the problem is. Using the *PP* data in order to update the *P* velocity model the best possible way, will lead to only a two-parameter estimation (ρ_s and γ).

REAL DATA RESULTS

In order to implement and test Stolt residual migration for converted waves, I use a 2D line from a 3D cube of the OBC data set of the Alba oil field. The 2D line is extracted from the 3D portion after geometry regularization (Rosales and Biondi, 2002).

The velocity models were provided by Chevron. I start with these velocity models. I first handle the *PP* section, perform Stolt residual migration on this section only and update the velocity model with a selection of combined values of ρ_p. After the *P* velocity model is updated, I perform the *PS* migration and residual migration; however, I do not scan over ρ_p values. I scan only over ρ_s and γ values.

The velocities vary both horizontally and vertically. Therefore, there will not be a single set of parameters to correct the entire section. The γ_0 value will be choosen at Alba's depth at the center of the section.

PP results

Figure 1 shows the migration result. Figure 2 shows three angle gathers. Observe the residual moveout in these angle gathers. This indicates errors in the velocity model.

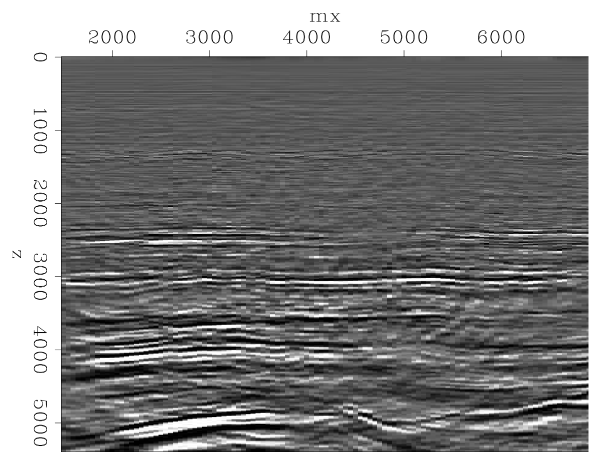

Figure 1: *PP* migration result with the original *P*-velocity model daniel1-ppmiga [CR]

I perform Stolt residual migration (Sava, 1999) over this migration result. There is not a single value of ρ_p that fixes the whole section. Figure 3 shows the same three angle domain common image gathers, as in Figure 2. Moreover, each angle domain common image gather corresponds to a different value of ρ_p, from left to right, $\rho_p = 0.98$ $\rho_p = 0.99$ and $\rho_p = 1.02$. Note how different events correct better for different ρ_p values.

By updating the velocity model with different ρ_p values at different depths and lateral positions, I perform a new migration. Figure 4 shows this final migration result. Figure 5 shows again the same different angle domain common image gathers for the migration result of Figure 4.

PS results

Figure 6 shows the *PS* migration result, using the updated *P* velocity model and the given *S* velocity model. Figure 7 shows three angle domain common image gathers for this migration result.

Figure 8 presents the residual migration results keeping the ρ_p value as 1, i.e, no changes in the *P*-velocity field, and a ρ_s value of 0.98. Figure 9 shows the angle domain common

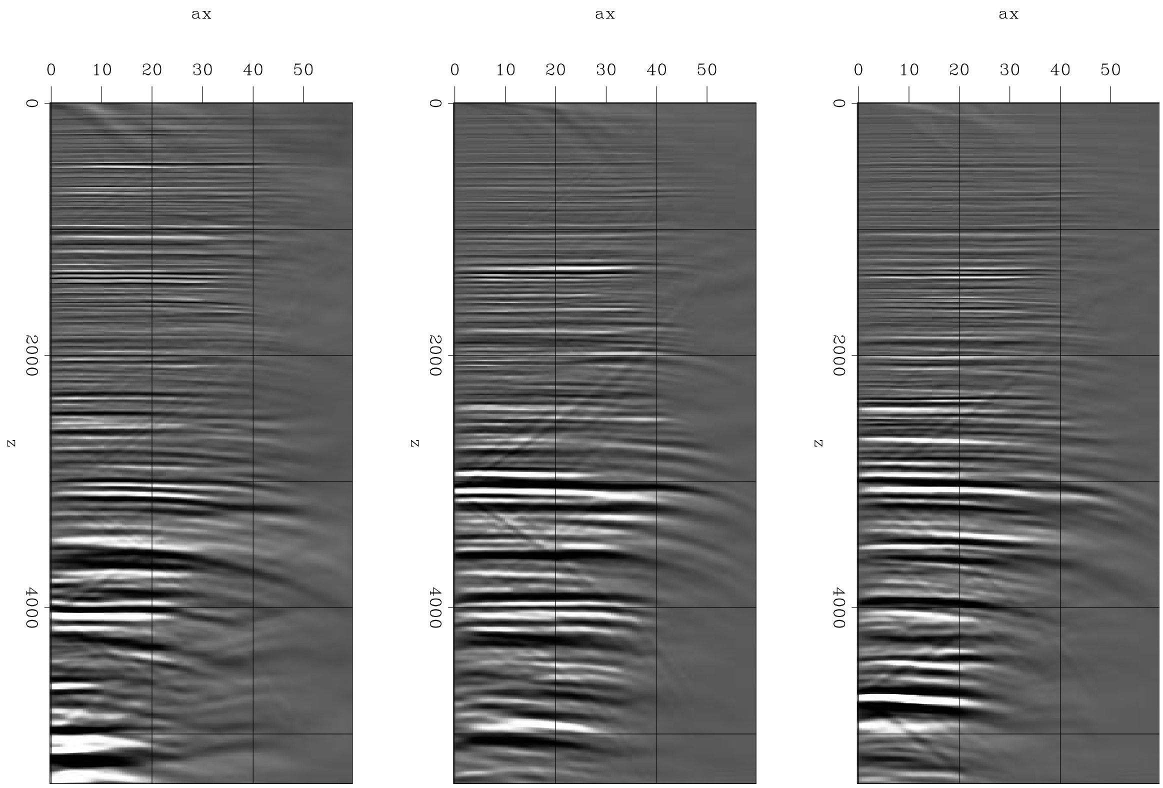

Figure 2: Three angle domain common image gathers for the migration result of Figure 1. They corresponds, from left to right, to a lateral position of 2500m, 4500m and 6500m. Observe the residual curvature. daniel1-ppmigb [CR,M]

image gathers for the residual migration process. These angle gathers are at the same position as in Figure 7, however, they correspond to ρ_s values of $\rho_s = 0.98$ $\rho_s = 0.99$ and $\rho_s = 1.02$.

The γ_0 value used for the PS residual migration is constant for the whole section, with a value of $\gamma_0 = 1.728709$. The γ_0 value was chosen at a depth of 1900m, which is the estimated depth of the Alba reservoir, and at the center of the section.

SUMMARY

I present the application of Stolt residual migration for converted waves on a real data set. Many challenges are involved in this application. The most important is the sparsity of the data. This problem is well addressed by Rosales and Biondi (2002).

In order to handle a 6D cube of information for a 2D prestack line after residual migration for converted waves, I freeze the ρ_p parameter after applying residual migration only on the *PP* section. A more robust technique to deal with all the parameters simultaneously is in progress.

Picking the parameter values is also a troublesome problem, Clapp (2002) presents some suggestions on how to deal with this problem on *PP* data only. A simultaneous picking might

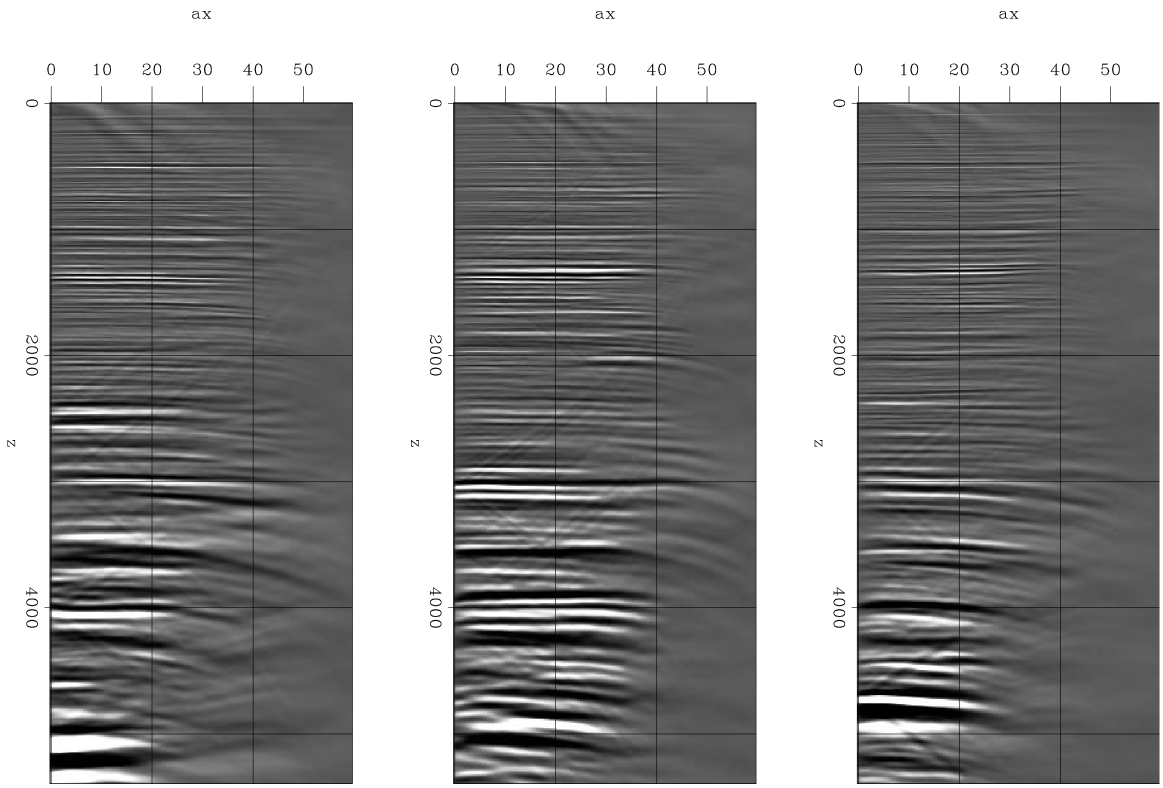

Figure 3: Angle domain common image gathers after Stolt residual migration. They corresponds to the same position as the angle gathers in Figure 2. Moreover, from left to right they also correspond to $\rho_p = 0.98$ $\rho_p = 0.99$ and $\rho_p = 1.02$ daniel1-ppsrm2 [CR,M]

be a solution.

Even though the theory of Stolt migration assumes constant velocity, Stolt residual migration can be safely applied to depth variant models, due to the dependency only on velocity ratios. This statement is also valid for multicomponent data.

REFERENCES

Clapp, R. G., 2002, Ray based tomography using residual Stolt migration: SEP–**112**, 1–14.

Rosales, D., and Biondi, B., 2002, Multicomponent data regularization: SEP–**112**, 97–108.

Rosales, D., Sava, P., and Biondi, B., 2001, Stolt residual migration for converted waves: SEP–**110**, 49–62.

Sava, P., 1999, Short note–on Stolt prestack residual migration: SEP–**100**, 151–158.

Sava, P., 2000, Variable-velocity prestack Stolt residual migration with application to a North Sea dataset: SEP–**103**, 147–157.

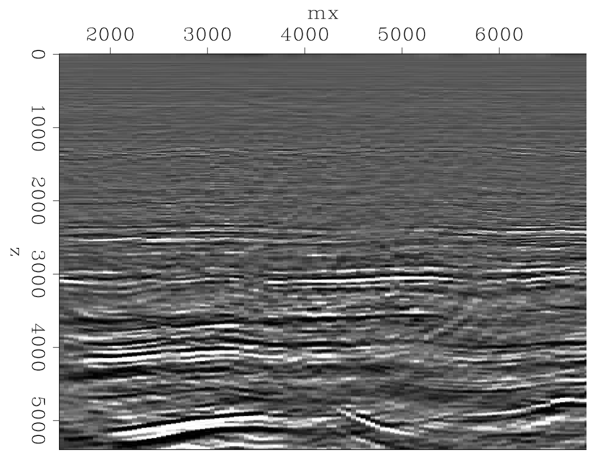

Figure 4: Migration result after updating the *P* velocity model with different values of ρ_p at different depth and lateral locations. daniel1-finalpp [CR,M]

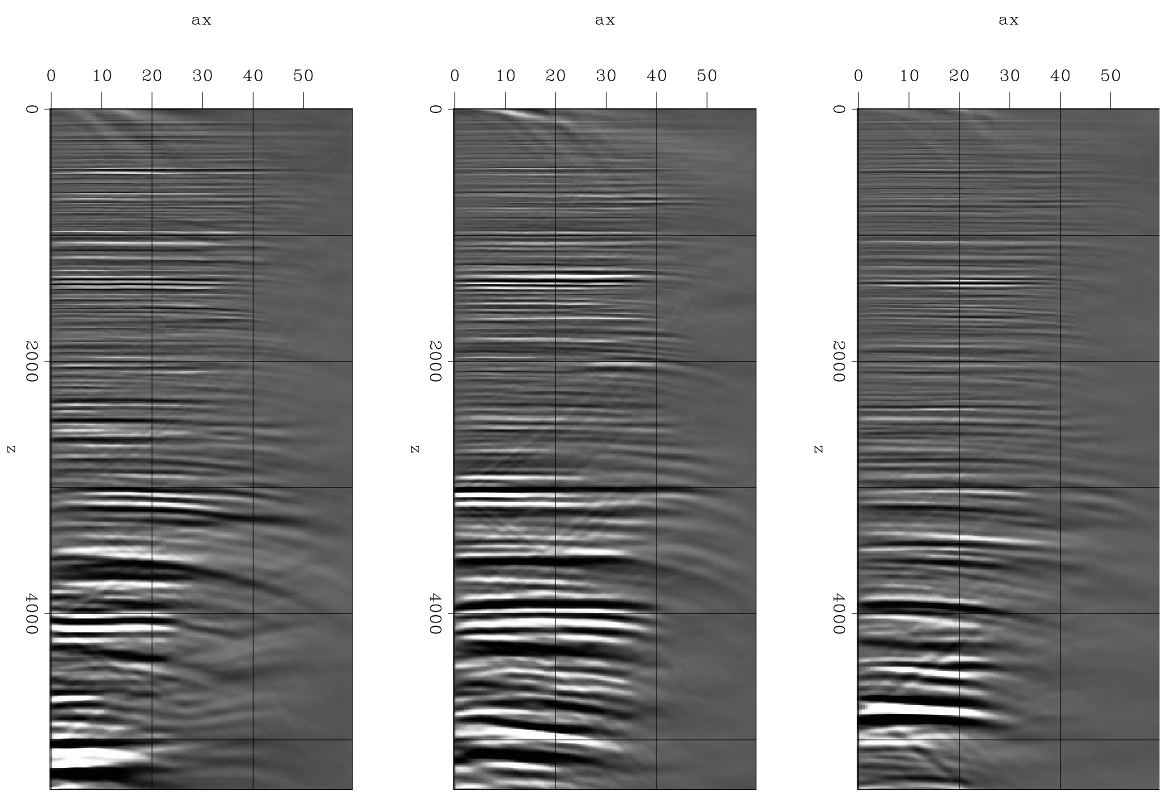

Figure 5: Angle domain common image gathers for the migration result of Figure 4 at the same position of Figure 2. daniel1-finalcag [CR,M]

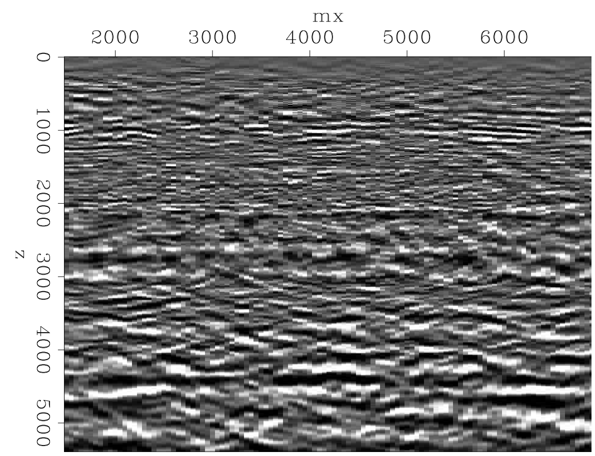

Figure 6: *PS* migration result with the updated *P* velocity model and the given *S* velocity model. daniel1-psmiga [CR]

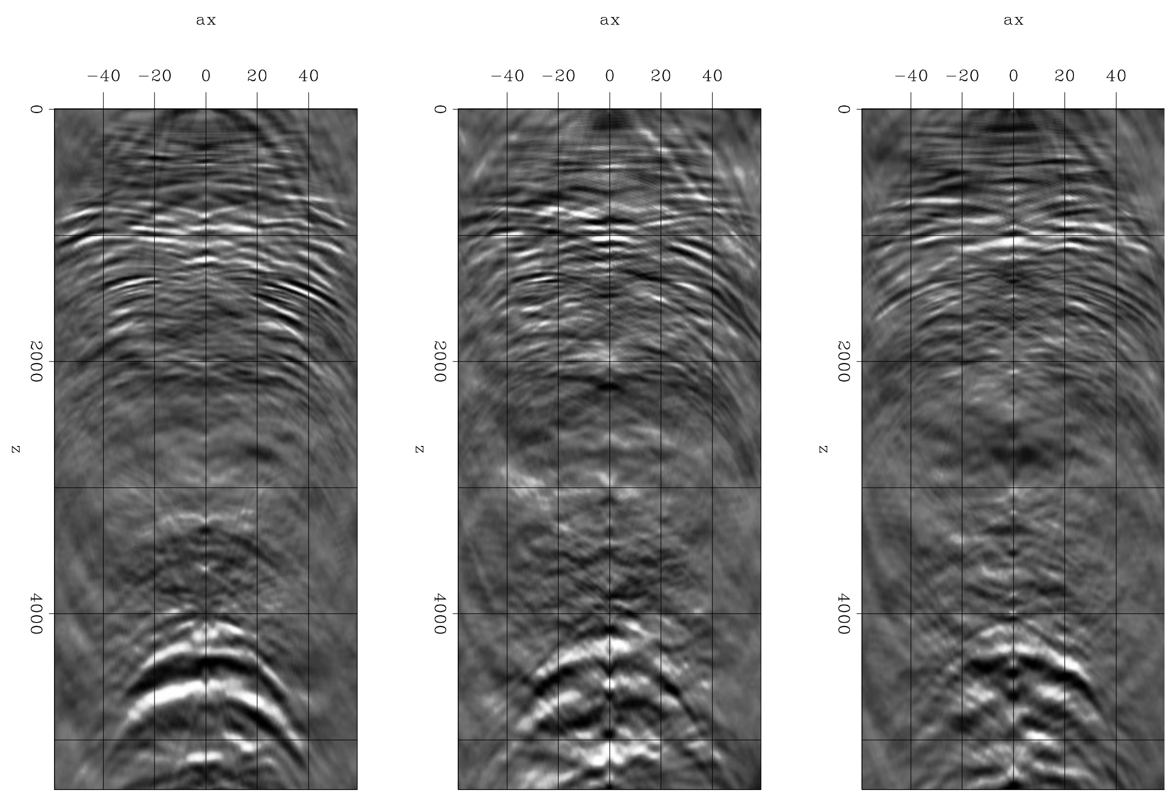

Figure 7: *PS* angle domain common image gathers. They corresponds, from left to right, to a lateral position of 2000m, 4000m and 5400m. Observe the significant residual curvature. daniel1-psmigb [CR,M]

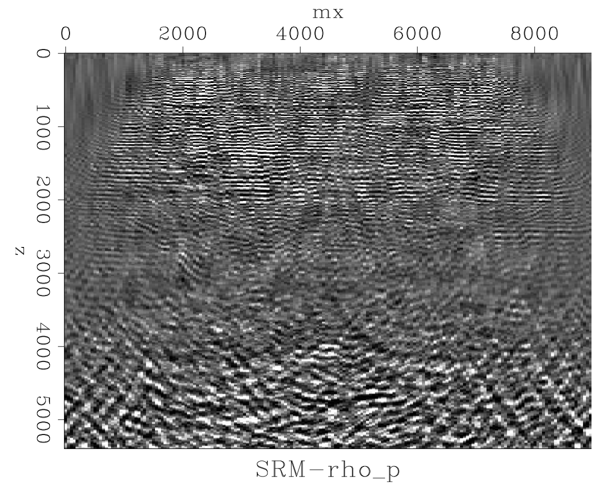

Figure 8: *PS* Stolt residual migration result daniel1-pssrm [CR,M]

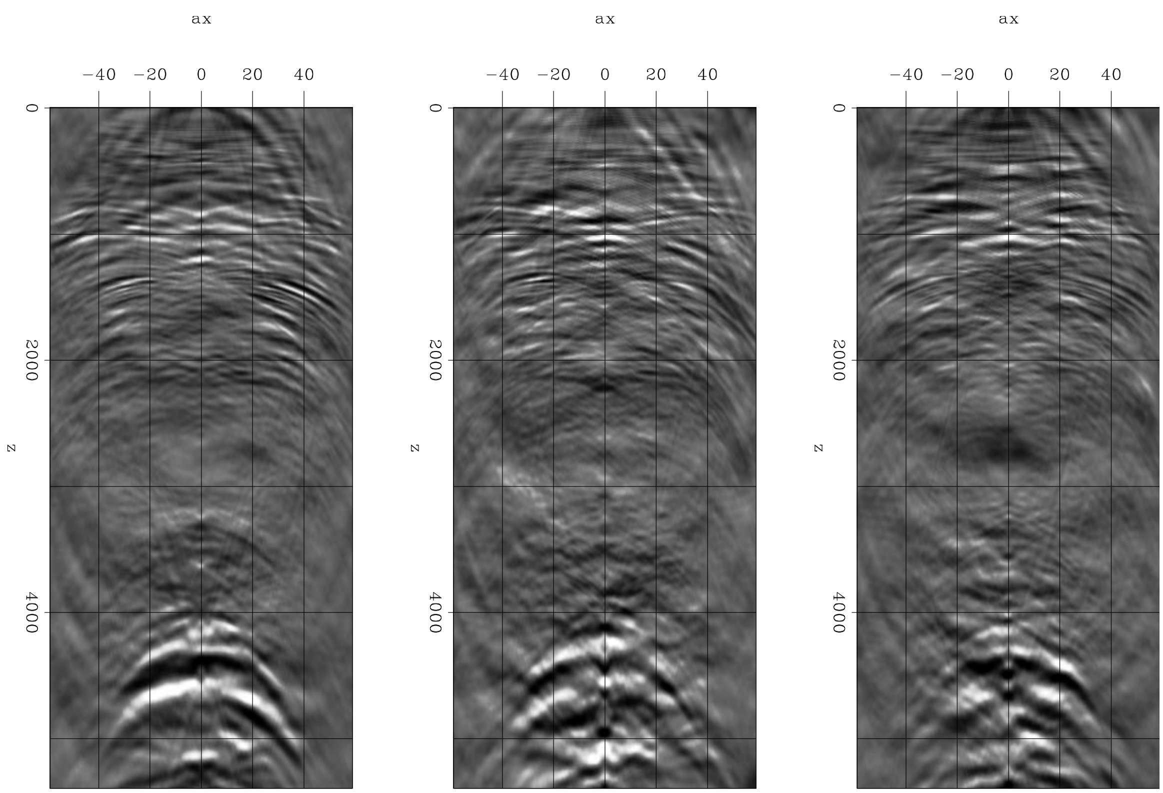

Figure 9: *PS* angle domain common image gathers after Stolt residual migration for converted waves. They are at the same location as in Figure 7 and corresponds to, from left to right, $\rho_s = 0.98$, $\rho_s = 0.99$ and $\rho_s = 1.02$. daniel1-pssrm2 [CR,M]